

INTRODUCTION TO AERMOD

by
Akula Venkatram

Goal

This chapter introduces the concepts that underlie dispersion modeling, and provides the reader with an overview of the approach used in formulating the *AMS/EPA Regulatory Model*, AERMOD, which is recommended by the USEPA for estimating the impact of new or existing sources of pollution on ambient air quality levels at source-receptor distances of less than 50 km. It replaces the ISC (EPA, 1995) model, which until November 2005 was the preferred model for regulatory applications at these distances.

Objectives

After reading this chapter, the reader should be able to do the following:

1. Explain the fundamentals of dispersion modeling.
2. Describe the variables that govern plume dispersion.
3. Explain the difference between the approaches used in the Industrial Source Complex (ISC) model and AERMOD.
4. Describe the processes that govern the atmospheric boundary layer.
5. Explain the relationship between turbulence and dispersion.
6. Explain the foundations of AERMOD.

Dispersion Modeling

The concepts that underlie the formulation of a dispersion model, such as AERMOD, can be illustrated by constructing a simple model to estimate ground-level concentrations associated with the surface release shown in Figure 1. The figure shows plume structure averaged over say half an hour, so that the irregular boundaries of the observed instantaneous plumes are smoothed out through time exposure. The concentrations

associated with an instantaneous plume are difficult to estimate, while a time averaged plume is more amenable to analysis.

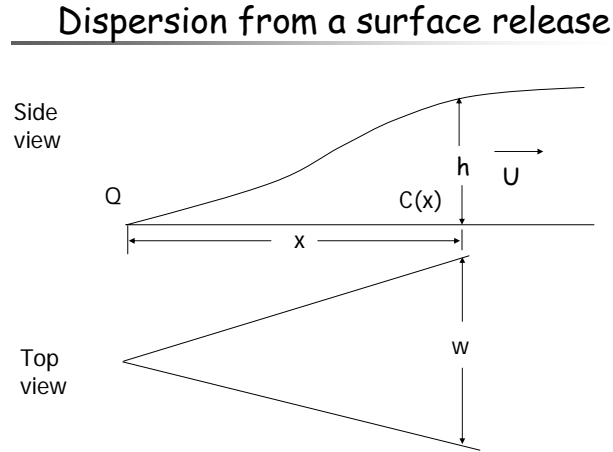


Figure 1: Schematic of plume dispersion from a surface release

Assume that pollutant release rate is Q gm/s. For simplicity, we take the pollutant to be well mixed both in the horizontal and the vertical through the cross-sectional area of the plume. At a distance, x , from the source, the cross-sectional area is the height, h , multiplied by the width, w . Then, the material passing through this area is $C(x)hwu$, where the wind speed, U , is taken to be constant over the height of the plume. If we assume that no material is removed by the ground, the emission rate, Q , has to be equal to the transport of material through the plume cross-section at any distance. This yields the following expression for the concentration, $C(x)$,

$$C(x) = \frac{Q}{Uhw}. \quad (1)$$

Although this is a highly simplified model of the real world, it contains the essentials of dispersion models used in regulatory applications. In fact, Equation (1) multiplied by a constant was the basis of the dispersion scheme proposed by Pasquill in 1961.

How do we determine the height and width of a plume when, in reality, the concentration is not uniform across the cross-section of the plume? Observations indicate that the time averaged concentration has distributions that are approximately Gaussian both in the horizontal as well as the vertical as seen in Figure 2.

Concentration distributions in the plume

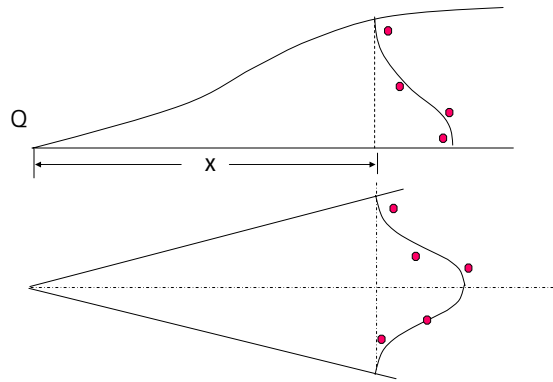


Figure 2: Measurements of concentrations at any height can be described approximately by bell shaped Gaussian distributions. The actual measurements might deviate significantly from the smooth curves.

The concentration distribution, $C(x,y,z)$, at any height can be described by

$$C(x,y,z) = C(x,0,0) \exp\left(-\frac{y^2}{2\sigma_y^2}\right) \exp\left(-\frac{z^2}{2\sigma_z^2}\right), \quad (2)$$

where y is the distance from the plume centerline, shown as a dotted line in Figure 2, and σ_y is the standard deviation of the horizontal Gaussian distribution. The second exponential in the equation describes the vertical distribution, where z is the height measured from the ground, and σ_z is the standard deviation of the vertical Gaussian distribution. The standard deviations of the distributions, σ_y and σ_z , are referred to the horizontal and vertical spreads of the plume. Notice that the actual concentration measurements might deviate significantly from the smooth curve of the formula.

We now have the terminology to describe the ISC model, the forerunner of AERMOD. We first describe some of the features of ISC and then relate them to the formulation of AERMOD. This approach is designed to facilitate readers who might be familiar with ISC to make the transition to AERMOD.

1.1 Dispersion in ISC

The Industrial Source Complex (ISC) model is based on the steady state Gaussian dispersion equation. If the ground is taken to be the reference height ($z=0$), with the x -axis of the co-ordinate system aligned along the wind direction at the source, empirical evidence indicates that the time averaged (typically one hour) concentration field can be described in terms of the Gaussian distribution (See Figure 3):

$$C(x, y, z) = \frac{Q}{2\pi U \sigma_y \sigma_z} \left[\exp\left(-\frac{(h_s - z)^2}{2\sigma_z^2}\right) + \exp\left(-\frac{(h_s + z)^2}{2\sigma_z^2}\right) \right] \exp\left(-\frac{y^2}{2\sigma_y^2}\right) \quad (3)$$

where x is the downwind distance, y is the cross-wind co-ordinate, z is the vertical coordinate, Q is the source strength (mass/time), h_s is the effective height of the source above ground, U is the time-averaged horizontal wind speed at source height, and σ_y and σ_z are the plume spreads normal to the mean wind direction.

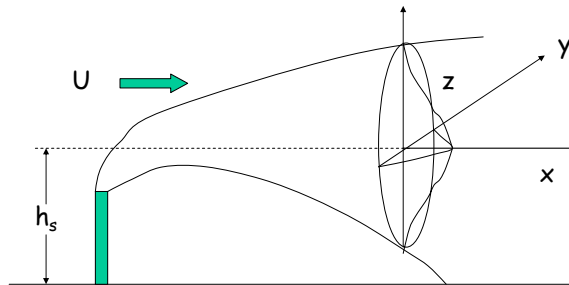


Figure 3: The idealized plume with concentration profiles described with Gaussian distributions.

In ISC, the plume spreads, σ_y and σ_z , are expressed as functions of distance from the source. These functions, referred to as dispersion curves, consist of two sets, one for releases in rural areas, and the other for urban conditions. Each set consists of 6 curves

corresponding to stability classes ranging from A to F, which in turn are keyed to routinely available meteorological observations. These dispersion curves are empirically derived from field studies, one of which was conducted in rural Nebraska, and the other in the St. Louis urban area. We will first describe these field studies, and then provide the background necessary to understand the basis of the stability classes. We can then justify the improvements incorporated in AERMOD to model dispersion.

The dispersion curves that apply to rural areas are referred to as Pasquill-Gifford-Turner (PGT) dispersion curves, which were developed about thirty years ago through empirical analyses of observations from field studies of dispersion in the surface boundary layer. The PGT dispersion scheme, proposed by Pasquill in 1961, are based observations made during the Prairie Grass experiment conducted in Nebraska in 1956. The experimental site in Nebraska was flat, covered with grass stubble 5-6 cm high; the effective roughness length was 0.6 cm. Meteorological measurements consisted of wind speed, temperature, and humidity at heights between 25 cm to 16 m on a tower. The experiment, conducted during July, August 1956, consisted of 70 runs. Each run, lasting 10 minutes, consisted of releasing SO₂ at a height of 46 cm (1.5 m for runs 63-68), and making concentration measurements at sampling arcs at distances of 50 m, 100 m, 200 m, 400 m, and 800 m from the release point. The concentration was measured at 1.5 m, except for the arc at 100 m where measurements were made on 6 towers at heights ranging from 0.5 m to 17.5 m.

The concentrations measured at 1.5 m were fitted to horizontal Gaussian distributions to obtain σ_y as a function of distance from the release. Then, the vertical spreads were inferred through Equation (2) by substituting the known values of centerline concentration, wind speed and computed σ_y . The variation of σ_y and σ_z as a function of distance from the source are the rural dispersion curves used in the ISC model. Note that these dispersion curves are based on measurements made at less than 1 km from the source. The variation of plume spreads for larger distances are based on extrapolations from a few measurements made in England.

The urban dispersion curves used in ISC are based on measurements made during the St. Louis study conducted over the period 1963-1965. The study consisted of a series of 26 daytime and 16 evening experiments in which fluorescent zinc cadmium sulfide particles

were released near ground level at two different locations. During the first year of the experiments the release was at ground-level in a relatively open area in a park located west of the downtown area. In the second year, the tracer was released from the top of a three storey building. These release locations were close to an area consisting of one to three storey buildings. The main downtown area, consisting of buildings with an average height of 40 m, was about 5 km away.

The daytime experiments were conducted between 10:00 and 14:00 CST, while the evening experiments were conducted between 21:00 and 22:00 CST. The release, which was typically 1 hour long, was sampled on arcs at 800 m to 16 km from the release point. Surface dose measurements were made at each arc near the anticipated plume centerline using a total of 30 to 50 samplers. The location of these samplers varied from experiment to experiment depending on the forecasted location of the plume. In nine experiments, dose measurements were made at various heights along a balloon tether about the expected plume centerline.

A meteorological network of three stations on the outer area of the sampling area and an instrumented television tower tracked wind, temperature, and relative humidity. A TV tower instrumented at three levels measured profiles of wind and temperature. Winds were profiled to a height of a kilometer using a single-theodolite, free or tethered radiosonde ascents, and transponder-equipped tetroons. The standard deviation of horizontal wind direction fluctuations, σ_θ , was estimated at 39 m and 140 m using variations of azimuth angle recorded on charts.

The horizontal plume spreads in the St. Louis study corresponded to the standard deviations of the observed surface concentration distributions on each of the sampling arcs. The vertical plume spreads were inferred by matching concentration estimates from a Gaussian dispersion model to observed surface concentrations. Briggs (1974) fitted analytical curves to the dispersion data presented by McElroy-Pooler (1968). These curves also used data from other urban tracer experiments conducted in Johnstown, Pennsylvania (Smith, 1967) and Ft. Wayne, Indiana (Csanady et al., 1967). Thus, Briggs's expressions attempt to describe dispersion of releases in a variety of urban settings. Briggs (1974) designed these urban curves to incorporate growth rates that were twice the rural values at short distances, and approach the rural values asymptotically.

These dispersion curves, although derived by Briggs, are referred to as the McElroy-Pooler curves to acknowledge the source of the underlying data.

As mentioned earlier, the set of dispersion curves used in ISC are mapped to stability classes, which in turn are functions for routine meteorological observations. These stability classes are related to the approach used in AERMOD to model dispersion. To see this relationship, we need some background in atmospheric turbulence and dispersion, which is presented in the next section. More details are provided in Chapters 2 and 3.

1.2 Turbulence in the Atmospheric Boundary Layer

Measurements of velocity made near the ground indicate that the three components of velocity, u , v , and w vary considerably in both space and time. The impact of this motion in the atmosphere on pollutant concentrations is most conveniently analyzed by assuming that the instantaneous velocity is the sum of two components: a mean velocity obtained by averaging the measured velocity over a time period and a fluctuating turbulent component. For the horizontal velocity in the x direction, this decomposition results in

$$u = U + u', \quad (4)$$

where U is the time averaged velocity, and u' is the turbulent component. Then, the behavior of material released into the atmosphere is modeled in terms of transport away from the source by the mean velocity, U , and dispersion in the three coordinate directions by the turbulent fluctuations. In other words, particles released in the turbulent flow have mean motion along the direction of U , but their locations in the horizontal and the vertical directions are only known with the precision governed by the standard deviations σ_y and σ_z , which in turn are related to the standard deviations of the turbulent velocities about the mean velocities. The standard deviations of the turbulent velocities in the two horizontal directions, x and y , and the vertical direction, z , are denoted by σ_u , σ_v , and σ_w .

Turbulent motion in the atmosphere, especially in the vertical direction, is most vigorous in the layer next to the ground. This layer, which can extend to heights of several kilometers, is known as the atmospheric boundary layer (ABL). Turbulent motion in the ABL is maintained by two mechanisms. The first mechanism is associated with the

interaction between the horizontal force exerted by one layer of air on an adjacent layer and the gradient of the mean velocity with height. This is referred to as the mechanical or shear production of turbulence. High mean velocities near the ground lead to high turbulent velocities because the velocity at the ground is zero, which means that a large mean velocity is associated with a large mean velocity gradient. The presence of obstacles such as trees and buildings also increases mechanical production of turbulence because these obstacles increase the horizontal forces that slow down the mean wind.

The second mechanism for turbulence production is related to buoyant air parcels originating from the ground heated by solar radiation. This mechanism is governed by the energy balance at the ground, which we discuss qualitatively next. The turbulent energy that is generated by these two mechanisms is ultimately converted by viscous dissipation into heat. More quantitative aspects will be examined in Chapter 2.

1.3 The Surface Energy Balance

Surface Energy Balance

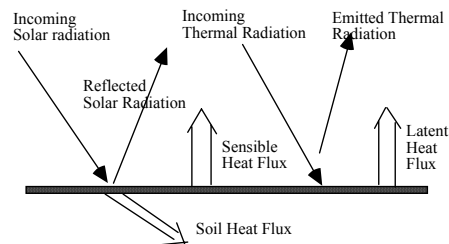


Figure 4: Components of energy fluxes at the ground air interface

At the interface between the soil and the atmosphere there is a balance between the incoming and outgoing fluxes of energy, as shown in Figure 4. During the daytime, the largest incoming stream is the short wave radiation from the sun, which refers to radiation with wavelengths less than $4 \mu\text{m}$; the peak of the solar spectrum is about $0.5 \mu\text{m}$. This incoming solar heat flux depends on the time of year and day, and the cloud cover. The fraction of the flux that is reflected by the ground is referred to as the albedo.

Snow has an albedo approaching unity, while typical urban surfaces have an albedo of 0.15.

The ground emits long wave thermal radiation corresponding to the temperature of the ground. Thermal radiation refers to wavelengths greater than $4\ \mu\text{m}$ with a peak around $10\ \mu\text{m}$. The atmosphere also emits thermal radiation, a fraction of which reaches the ground. The incoming thermal radiation depends on the effective temperature of the atmosphere, which is generally smaller than that of the ground. This implies that the outgoing thermal radiation is generally larger than the incoming atmospheric thermal radiation. This deficit is largest during clear skies, and smallest during cloudy skies. This is because clouds, especially at small heights, have temperatures that are higher than the effective atmospheric temperature. Clouds increase the downward thermal radiation by emitting radiation at a higher temperature than the effective atmosphere.

The radiative energy flux reaching the ground is balanced by three components: 1) heat transfer into or from the boundary layer, 2) energy transfer to evaporate water at the surface, and 3) heat transfer from or into the soil. The first component is called sensible heat flux, and the second is referred to as latent heat flux. The ratio of the sensible to latent heat flux is called the Bowen ratio.

Sensible heat is transferred from the ground to the boundary layer when parcels of air next to the heated ground acquire higher temperatures than their surroundings and become buoyant. These parcels rise vertically inducing vertical motion and pressure differences that produce turbulent motion in all three directions. These rising parcels transfer their energy to their surroundings, and are thus responsible for transfer of heat from the heated ground to the boundary layer above. Latent heat transfer is associated with the energy carried away by water vapor when water at the ground is first converted into water vapor and then transferred to the dryer boundary layer. The last component of the energy balance is the soil heat transfer associated with conduction through the soil in response to temperature gradients in the soil.

1.4 Adiabatic Lapse Rate and Static Stability

When an air parcel moves vertically in the atmosphere, its temperature changes even if it does not exchange heat with its surroundings. To understand this, we note that the

pressure decreases with height in the atmosphere because the pressure at any height is essentially the weight of the unit area air column above that height. The maximum pressure at the ground corresponds to the weight of the entire column overhead, and the pressure decreases as we go up because the column above decreases in height.

When an air parcel moves upwards, it encounters a decrease in pressure. This decrease leads to expansion of the air parcel, which in turn leads to cooling. Conversely, when a parcel moves downwards it undergoes compressive heating because the pressure increases as the height decreases.

When the parcel moves without exchanging heat with its surroundings, it is said to undergo an adiabatic process. The temperature change associated with this adiabatic movement represents can be used to examine the static stability of the atmosphere. This is facilitated by defining a quantity called potential temperature that accounts for the effects of pressure changes on temperature when a parcel moves vertically. The potential temperature, θ , of a parcel is that that attained by a parcel at temperature, T , and pressure, p , when it is moved adiabatically to a reference pressure, p_0 .

$$\theta = T \left(\frac{p_0}{p} \right)^{R_a / C_p}, \quad (5)$$

where p_0 is taken to be $=10^5 \text{ N/m}^2$, a quantity that is referred to as a bar in atmospheric literature, $R_a=287 \text{ kJ}/(\text{kg.K})$ is the gas constant of air, and $C_p=1000 \text{ kJ}/(\text{kg.K})$ is the specific heat of air.

It turns out that the potential temperature of an air parcel remains constant during adiabatic vertical motion. On the other hand, the temperature, T , decreases with height at a rate called the adiabatic lapse rate, which is approximately $10^0 \text{ C per } 1000 \text{ m}$.

Atmospheric Stability

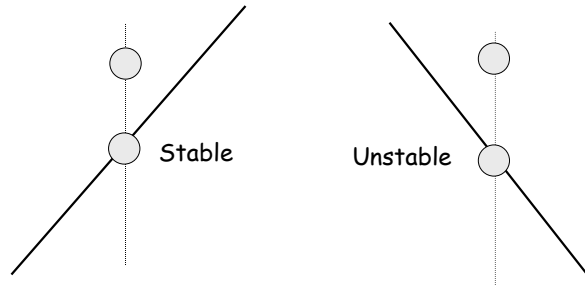


Figure 5: How potential temperature is related to stability of the atmosphere

The concept of potential temperature can be used to examine the stability of the motion of a parcel in an atmosphere. The solid lines in the two figures of Figure 5 represent profiles of potential temperature in the atmosphere, and the shaded circles represent air parcels whose stability is being examined. Consider the right figure, which shows the potential temperature decreasing with height. Let us move an air parcel vertically in this atmosphere, and assume that this motion is adiabatic. This means that during this motion, the potential temperature of the parcel remains constant. The parcel's potential temperature is shown as a dotted line.

When the air parcel is moved upwards to its new position, it is warmer and hence less dense than its surroundings. It is thus subject to an upward buoyancy force which continues to push it away from its initial position. The motion of the air parcel is also unstable when it is pushed downwards. The air parcel is denser than its surroundings, and thus continues to sink away from its initial position; when the potential temperature decreases with height, the atmosphere is unstable to air motion. Any motion is amplified in such an atmosphere.

The left figure shows a stable atmosphere, which resists vertical motion. If a parcel is moved upwards, it is denser than its surroundings and falls back to its original position. When moved downwards, the parcel is lighter than the surrounding atmosphere, and thus rises back to its original position.

When the potential temperature decreases with height or is uniform, the atmosphere is said to be unstable because vertical motion is enhanced in such an atmosphere. A positive potential temperature gradient is said to be stable because it inhibits vertical motion. Chapter 2 provides a more detailed explanation of these concepts. We mention it here primarily because this concept of 'static' stability is often confused with the stability classes used in the Pasquill dispersion scheme discussed later.

1.5 Vertical Structure of the Atmospheric Boundary Layer

Because vertical heat flux results in motion of air parcels, it is associated with production or destruction of turbulence. It is considered positive when it is directed away from the ground. Under these circumstances, the temperature decreases with height as air parcels heated by the ground accelerate upwards. Hence, a negative temperature gradient with height leads to buoyancy production.

Conversely, a positive temperature gradient, when the temperature increases with height, inhibits turbulence production. A positive temperature gradient occurs during the night when the ground cools because the outgoing thermal radiation from the ground exceeds the incoming thermal radiation from the atmosphere. This thermal radiation deficit is made up through turbulent heat transfer from the boundary layer to the ground, and heat transfer from the soil to the surface. Heat transfer towards the ground is denoted negative and is associated with a positive temperature gradient. Thus, a negative heat flux results in destruction of turbulence.

We said that the negative heat flux is caused by the deficit between the outgoing thermal radiation from the ground and the incoming thermal radiation from the atmosphere. If the sky is cloud free, the incoming thermal radiation reflects the low temperatures of the upper atmosphere and the radiation deficit is large. On the other hand, low level clouds at temperatures that are high relative to the upper atmosphere can reduce the deficit by emitting more downward thermal radiation. Thus, a clear sky is associated with more surface cooling than a cloudy sky. Thus, destruction of turbulence is most pronounced during clear skies.

The height of the boundary layer depends on turbulence production through the mechanisms discussed in the preceding paragraphs. During the day, buoyancy and

mechanical production of turbulence reinforce each other, and lead to increase in the height of the boundary layer from small values at sunrise. The boundary layer height increases with time of day as long as the heat flux is directed upwards from the ground into the boundary layer. The rate at which the boundary layer grows is determined by the surface heat flux and the temperature gradient in the layer above the boundary layer. The temperature gradient is usually positive- temperature increases with height- above the boundary layer, and it inhibits the growth of the boundary layer. The maximum boundary layer height, which occurs at sunset, decreases as this temperature gradient increases. Because turbulence is generated by buoyancy as well as by shear (mechanical production), there is vigorous mixing through the depth of the boundary layer. For this reason, the daytime boundary layer is often referred to as the mixed layer. Because of buoyancy induced mixing, properties such as wind speed and pollutant levels are relatively constant within the mixed layer.

Figure 6 shows the typical time evolution of the height of the boundary layer. Once the sun rises, the relatively shallow nighttime boundary layer grows rapidly as surface heating by the sun leads to buoyancy production of turbulence. The boundary layer grows throughout the day at a rate that depends on the temperature gradient of the layer that the boundary layer is eroding from below. The growth stops at sunset when buoyancy production is switched off. After this point, the boundary layer height decreases rapidly to a much smaller height corresponding to the nighttime boundary layer. The boundary layer height varies through the night in response to the balance between shear production and buoyancy destruction of turbulence. The maximum daytime boundary layer height is of the order of 1000 m, while the nighttime boundary layer height is of the order of 100 m.

ABL Evolution

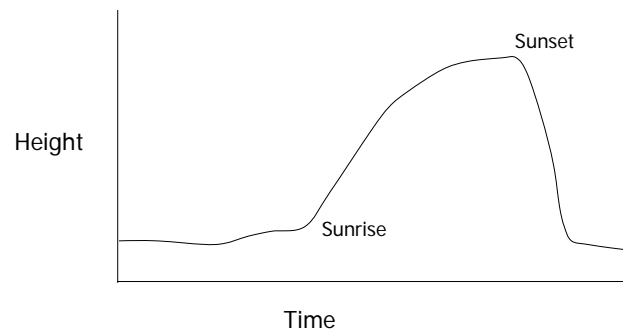


Figure 6: Variation of the atmospheric boundary layer as a function of time of day.

During the night, the heat flux in the atmosphere is generally negative, that is towards the ground. So the heat fluxes from the atmosphere as well as from the soil make up for the deficit in the net thermal radiation at the ground. Remember that there is no solar radiation during the night. This negative flux (positive temperature gradient) inhibits the production of turbulence by shear, and the resulting turbulence levels are several times smaller than those during the daytime. The boundary layer height is much smaller because of this competition between shear production and buoyancy and viscous destruction of turbulence. The relatively small mixing in this boundary layer allows the formation of sharp gradients in properties such as wind speed and temperature, both of which increase with height in the boundary layer.

Figure 7 shows the variation of the potential temperature in the daytime and nighttime boundary layers. During the night, the potential temperature generally increases with height near the ground, and the temperature gradient becomes much smaller aloft. In the daytime, the potential temperature gradient is negative near the ground and is small through the bulk of the boundary layer. The boundary layer can be capped by an inversion, which is a shallow layer in which the potential temperature increases by several degrees. This capping inversion usually marks the height at which vertical mixing ceases.

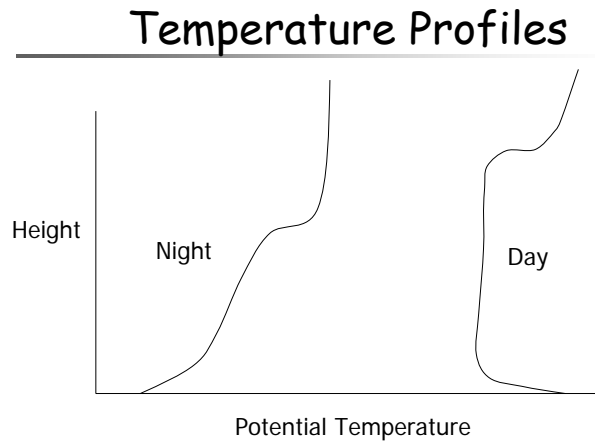


Figure 7: Vertical profiles of potential temperature in the daytime and nighttime boundary layers

Figure 8 shows the expected vertical variation of the mean wind and the standard deviation of vertical velocity fluctuations in the daytime and nighttime atmospheric boundary layers. The mean wind profile usually has a larger vertical gradient during the night than during the day, when vigorous turbulence mixes properties through the depth of the boundary layer.

Generally, turbulent velocities decrease with height in the nighttime stable boundary layer because shear production, which maintains turbulence, is a maximum near the ground. During the daytime, buoyancy production operates through the bulk of the boundary layer, and the turbulence levels are relatively uniform through the boundary layer, and then decrease rapidly near the top of the mixed layer.

Velocity and Turbulence Profiles

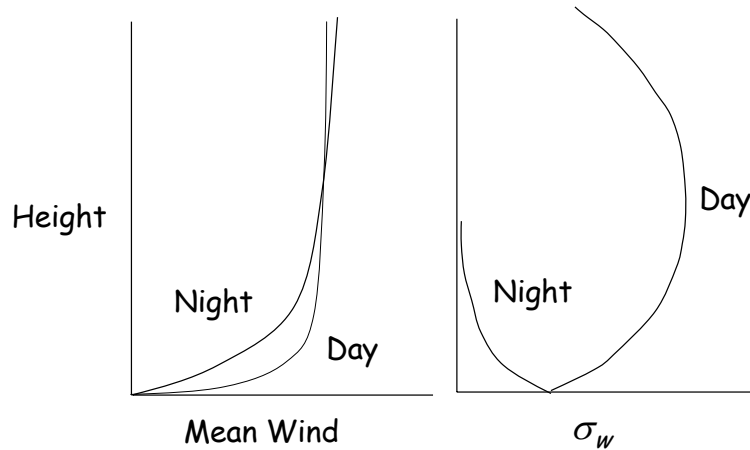


Figure 8: *Vertical profiles of mean wind and vertical turbulent velocities in the daytime and nighttime boundary layers*

1.6 Summary of the Properties of the Atmospheric Boundary Layer

Let us recall the main points of the discussion of the atmospheric boundary layer:

1. The motion in the atmosphere can be considered to consist of the sum of a time or space averaged mean velocity and a turbulent velocity. The turbulent velocities are described in terms of their statistics, the most important of which from the point of dispersion are the standard deviations of the velocities.
2. Turbulence is generated through two mechanisms: 1) shear production associated with the interaction of drag forces with mean velocity gradients, and 2) buoyant production associated with upward heat flux originating from the heated ground, or when cold air is transported over a warmer surface. Turbulence can be destroyed when the heat flux is negative (towards the ground) during nighttime conditions when the surface cools to a temperature below that of the overlying air. Turbulence is ultimately converted into heat by viscous dissipation.
3. Turbulence levels in the daytime boundary layer are much higher than those in the nighttime boundary layer because buoyancy and shear production act together

during the day, while shear production is counteracted by buoyancy destruction during the night.

4. The daytime boundary layer generally grows throughout the day reaching its maximum value around sunset. The nighttime boundary does not show this monotonic behavior, but varies in response to mean speed, which governs shear production of turbulence. The nighttime boundary layer height is about one-tenth that of the maximum daytime boundary layer height.
5. Mean velocity and temperature profiles have much smaller gradients in the daytime boundary layer than in the nighttime boundary layer because there is much more turbulent mixing during the daytime.
6. In the bulk of the daytime boundary layer, which is often referred to as the mixed layer, the temperature decreases with height at a rate called the adiabatic lapse rate, which is about 10°C per 1000 m. This temperature decrease is related to the cooling or heating that occurs when an air parcel moves vertically in a boundary layer with a vertical pressure gradient.

We now have the background necessary to understand the mechanisms that govern dispersion in the atmospheric boundary layer.

1.7 Stability Classes and Dispersion in the Pasquill Scheme

Recall that dispersion refers to spread of a plume through turbulent motion as material is advected or transported by the mean wind. To see how dispersion can be related to turbulence, consider a single particle that follows wind motion. For simplicity, assume that its velocity can be resolved into a mean component U and a vertically directed turbulent velocity, w . Let us now follow the motion of the particle over a time interval, t , during which the turbulent velocity, w , does not change appreciably. As the parcel moves a horizontal distance Ut , it is dispersed vertically through a distance wt . If the particle moves through a horizontal distance, x , from the source, the time of travel, $t=x/U$, which means that the vertical displacement of the particle can be written as wx/U . It can be shown that the standard deviation of the vertical position of particles originating with different turbulent velocities is given by:

$$\sigma_z = \sigma_w t = \frac{\sigma_w}{U} x, \quad (6)$$

where σ_w is the standard deviation of the vertical velocity fluctuations. The term σ_w/U is called the turbulent intensity. It turns that this simplified model of dispersion is an adequate approximation for dispersion when the plume is embedded in the upper part of the daytime boundary layer. We will examine more realistic expressions for dispersion in the next chapter. The main value of this simple expression is that it reveals the role of the turbulent intensity, σ_w/U , in dispersion: plume spread increases as turbulent intensity increases.

The Pasquill scheme, shown in Table 1, establishes relationships between meteorological observations of wind speed measured at 10 m, solar insolation, and cloudiness to stability classes ranging from A to G. It turns out that a stability class is an indicator of the turbulent intensity, which allows one to map a stability class to a dispersion curve obtained from the field studies discussed earlier. To see the relationship between stability class and turbulent intensity, recall that:

1. An increase in solar insolation increases turbulence levels associated with buoyant production of turbulence. Thus, keeping the wind speed constant and increasing solar insolation leads to an increase in turbulent intensity, and hence dispersion.
2. Solar insolation decreases with increase in cloud cover.
3. Keeping the solar insolation constant, and increasing the wind speed generally leads to a decrease in turbulent intensity even though increasing the wind speed leads to increased turbulence associated with shear production. This is because the effective turbulence levels seen by a dispersing plume is dominated by buoyancy produced turbulence.
4. During the night turbulence levels are controlled by the competition between shear production and buoyancy and viscous destruction. At low wind speeds and clear skies, shear production is low, and surface cooling is high, so that the turbulent intensity is small. The turbulent intensity increases with wind speed.

5. The presence of clouds increases the downward thermal radiation, and thus decreases surface cooling. This implies that increasing cloud cover at constant wind speed increases turbulent intensity and hence dispersion.

The relationships described in the preceding five points are embodied in the Pasquill scheme of Table 1. Class A, associated with the largest dispersion rate curve, occurs when solar insolation is strong and the wind speed is less than 2 m/s. As the wind speed increases, the stability class ranges from A to C. As the insolation decreases from strong to slight, the turbulent intensity decreases as the stability class ranges from A to D. The class D corresponds to neutral conditions when turbulence levels are dominated by shear production.

Table 1. Pasquill stability classification scheme

Wind speed at 10 m (m s ⁻¹)	Insolation			Night	
	Strong	Moderate	Slight	Thinly overcast or $\geq 4/8$ low cloud	
				$\leq 3/8$ cloud	
< 2	A	A-B	B	—	—
2-3	A-B	B	C	E	F
3-5	B	B-C	C	D	E
5-6	C	C-D	D	D	D
> 6	C	D	D	D	D

PGT Dispersion Scheme

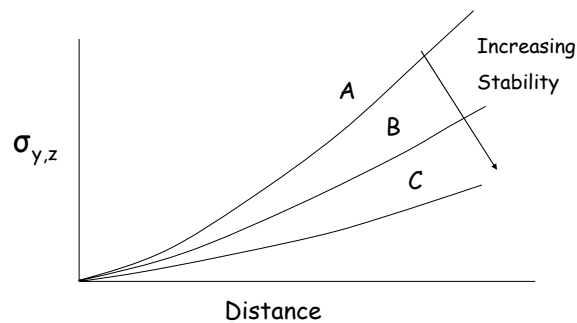


Figure 9: The relationship between PGT stability classes and plume spreads, σ_y and σ_z , as a function of distance from the source. .

During nighttime conditions, winds greater than 6 m/s result in neutral conditions. As the wind speed decreases for cloud cover less than 3/8, the turbulent intensity decreases as indicated by the stability class going from D to E. An increase in cloud cover keeps the stability class at D even when the wind speed is at 3 m/s. When the wind speed is less than 2 m/s, the associated stability class G, shown as a dash in Table 1, indicates very low turbulent intensities.

Pasquill's dispersion scheme was modified slightly by Gifford (1961) who converted the original formulation for dispersion into the more familiar plume spreads used in the Gaussian equation (1). Turner (1970) converted the qualitative description of solar insolation into ranges of solar elevation angle and cloud cover. This is why the Pasquill scheme is generally referred to as the Pasquill-Gifford-Turner (PGT) scheme.

We see that the Pasquill dispersion scheme consists of a semi-empirical method to estimate the stability class through meteorological observations. The stability class, as shown earlier, is an indicator of turbulent intensity. It is the relationship between turbulent intensity and dispersion that allows the scheme to map stability classes to dispersion curves derived made from measurements made during field studies discussed earlier. We see that the Pasquill scheme provides a sound foundation for estimating dispersion, and it is the reason for its use for the past 40 years.

However, the Pasquill scheme suffers from several disadvantages:

1. The relationships between meteorological observations and the variables, such as turbulent intensity, that control dispersion are semi-empirical. They are based on a small number of field studies involving surface releases, and are thus unlikely to apply to conditions different from these field studies.
2. The six distinct stability classes, A to F (G is rarely used), do not reflect the continuous nature of turbulent intensities, as well as the range of possible values.
3. It does not account for variations in surface properties, such as roughness length and albedo, which can play a major role in determining the relationship between meteorological observations and the turbulence properties that control dispersion.
4. The scheme-stability classes and dispersion curves- does not account for vertical variation of turbulent properties relevant to dispersion. It applies primarily to near surface releases, and is unlikely to provide an adequate description of releases in the middle of the boundary layer.

Since Pasquill first proposed his dispersion scheme in 1961, our understanding of micrometeorology and dispersion have advanced considerably. AERMOD incorporates these advances to overcome the problems that we have identified in the Pasquill scheme. The next section provides a brief description of AERMOD and its associated meteorological processor, AERMET. This provides the introduction to more detailed treatments in Chapters 2 and 3.

1.8 Meteorology and Dispersion in AERMOD

We saw earlier that estimating plume spread requires information on the statistics of the turbulent velocities in addition to the mean properties of the atmospheric boundary layer. The Pasquill scheme does not estimate turbulent velocities directly but provides a surrogate for the turbulent intensity through the stability class. The stability class approach has limitations that we discussed in the last section. AERMOD overcomes these problems using two steps:

1. It uses available meteorological observations as inputs to models of the atmospheric boundary layer to construct vertical profiles of wind, temperature,

and turbulent velocities in the atmospheric boundary layer. This task is accomplished using a processor called AERMET.

2. The outputs of AERMET are used in AERMOD to estimate concentrations of pollutants released from a variety of sources. AERMOD does not use empirical dispersion curves, proposed by Pasquill (1961) and Briggs (1974), as ISC does. It uses the micrometeorological variables from AERMET to construct dispersion curves on the basis of current understanding of dispersion. We point out that these dispersion curves are completely consistent with those used in ISC. However, unlike ISC, the dispersion formulations apply to elevated as well as surface releases.

The minimum inputs to AERMET are 1) wind at one level, 2) temperature at one level, 3) cloud cover, and 4) an early morning upper air sounding. In addition, AERMET requires information on surface roughness, albedo, and Bowen ratio. This information, coupled with meteorological inputs 2) and 3), are used in a surface energy balance to estimate the sensible heat flux, which in turn is used to estimate the surface shear stress exerted by the wind speed. The sensible heat flux as a function of time is then used to compute the mixed layer height during the course of the day. The upper level temperature sounding provides the temperature gradient above the mixed layer, which controls the rate of growth of the mixed layer. The nighttime boundary layer is governed by the computed surface shear stress.

The surface parameters, sensible heat flux and surface shear stress, and the boundary layer height are used in boundary layer models to construct the profiles of wind, temperature, and turbulent velocities required by AERMOD. AERMET can also incorporate measured values of these parameters in these profiles.

AERMOD uses the meteorological information supplied by AERMET in dispersion models that reflect the state of the art. Unlike ISC, AERMOD explicitly accounts for the variation of meteorological parameters with height by defining effective values that represent averages over the plume depth. Some of the features included in AERMOD are:

1. Enhanced dispersion in urban areas caused by increased surface roughness and heat flux.
2. Treatment of downwash associated with buildings.
3. Inclusion of models to account for dispersion caused by updrafts and downdrafts in the daytime boundary layer. The Gaussian distribution in the vertical does not provide an adequate description of the concentration distribution.
4. Consistent treatment of surface and elevated releases.
5. Treatment of terrain effects on dispersion. Plumes are allowed to impact on the terrain when the flow does not have energy to surmount the hill.

In chapter 2 of this manual, we will go into the details of the mean and turbulent structure of the atmospheric boundary layer. Chapter 3 will deal with the formulation of AERMOD.

REFERENCES

- Barad M. L., 1958: Project Prairie Grass--A field program in diffusion, Vols I and II. Geophysical Research Paper No. 59, Air Force Cambridge Research Center, Bedford, Massachusetts, NTID PB 151424, PB 1514251.
- Briggs, G.A., 1974: Diffusion estimation for small emissions. In ERL, ARL USAEC Report ATDL-106, U.S. Atomic Energy Commission, Oak Ridge, Tennessee.
- Calder K. L., 1949: Eddy diffusion and evaporation in flow over aerodynamically smooth and rough surfaces: a treatment based on laboratory laws of turbulent flow with special reference to conditions in the lower atmosphere. *Q. Jl Mech. Appl. Math. (Oxford)* 2, 153.
- Cramer H. E., 1957: A practical method for estimating the dispersal of atmospheric contaminants. In Proc. 1st Nat. Conf. Appl. Met., Hartford, Connecticut, October, 28-29, Boston, Massachusetts, p. C-33.

- Csanady, G.T., Hilst, G.R., Bowne, N.E., 1967: The diffusion from a cross-wind line source at Fort Wayne, Indiana. Unpublished Report, Travelers Research Center, Hartford, CT.
- EPA, 1995: User's guide for the Industrial Source Complex (ISC3) dispersion models. Volume II-Description of model algorithms. Report No. EPA-454/9-95-003b, U.S. Environmental Protection Agency, Office of Air Quality Planning and Standards, Emissions, Monitoring and Analysis Division, Research Triangle Park, North Carolina 27711, September 1995.
- Gifford F. A., 1961: Use of routine meteorological observations for estimating atmospheric dispersion. Nucl. Safety 2, 47-51.
- McElroy, J. L. and Pooler, F., 1968: The St. Louis dispersion study-volume II-analysis. National Air Pollution Control Administration, Pub. No. AP-53, US DHEW Arlington, 50 pages.
- Pasquill F., 1961: The estimation of the dispersion of windborne material. Meteor. Mag. 90, 33-49.
- Smith, D.B., 1967: Tracer study in an urban valley (Johnstown, Pennsylvania).M. S.Thesis in Meteorology, Pennsylvania State University, University Park, PA.
- Turner D. B., 1970: Workbook of Atmospheric Dispersion Estimates. USEPA, ASRL, Research Triangle Park, North Carolina.